STREAK CAMERA PSF OPTIMISATION AND DUAL SWEEP CALIBRATION FOR SUB-ps BUNCH LENGTH MEASUREMENT

L.M. Bobb, A.F.D. Morgan, G. Rehm, Diamond Light Source, Oxfordshire, U.K.

Abstract

Streak cameras are commonly used for bunch length measurement. In normal beam modes, bunch lengths are on the order of 10 ps. For the study of coherent synchrotron radiation, a low alpha single bunch beam mode is implemented with bunch lengths as small as 1 ps and beam current in the tens of μA. In order to reliably measure such a short bunch at low beam currents, the input optics for the streak camera must be optimised for sufficient incident light intensity and high resolution in both sweep directions. This is achieved through the use of reflective input optics in which a pinhole is imaged to provide a small circular PSF. Furthermore, to precisely measure the bunch length the calibration of the dual sweep must be known. Here we describe a calibration method using electrical delays to incorporate calibration information within streak camera images.

INTRODUCTION

Diamond Light Source (DLS) is a third generation synchrotron light source providing high brilliance x-ray beams for user experiments. Nominally a 3 GeV, 300 mA, 900-bunch electron beam is circulated in the storage ring with a revolution period of 1.8 μs. In this normal beam mode the momentum compaction factor α is 1.7×10^{-4} which, given the synchrotron frequency $f_s = 2.5$ kHz and relative energy spread $\sigma_\epsilon = 10^{-3}$ with Eq. 1, has zero current bunch length $\sigma_{bunch} \approx 10$ ps [1].

$$\sigma_{bunch} = \frac{\alpha}{2\pi f_s}\sigma_\epsilon \tag{1}$$

In the low alpha beam mode the electron bunch length is reduced to a few picoseconds. Due to the corresponding reduction in x-ray pulse duration, the temporal resolution used for pump-probe or time-of-flight experiments is improved. Furthermore the reduction in bunch length extends the wavelength range in which the electron bunch emits coherently towards the THz/far infrared region of the electromagnetic spectrum [2].

For the low alpha beam mode where $\alpha = 10^{-5}$, $f_s = 0.6$ kHz and $\sigma_\epsilon = 10^{-3}$ and using Eq. 1, the bunch length $\sigma_{bunch} \approx 2.6$ ps [1, 2].

To measure the longitudinal bunch profile and length, images of the synchrotron radiation (SR) pulses are acquired using a dual sweep streak camera (SC) from Optronis GmbH [3]. The fast deflection unit employs a synchroscan frequency of 250 MHz. This signal is provided to the SC by dividing the 500 MHz master oscillator frequency.

In order for the SC to measure these picosecond bunch lengths at bunch currents of tens of μA, the input optics for the SC must be optimised and the dual sweep calibration must be accurately measured. This report describes the implementation of reflective input optics including a pinhole to ensure maximum light intensity and smallest Point Spread Function (PSF) spot size for high resolution measurements, and presents a method for the dual sweep calibration of the SC using electrical delays.

EXPERIMENTAL SETUP AND ANALYSIS PROCEDURE

The Visible Light Extraction (VLE) system brings visible SR from a bending magnet in the storage to the diagnostics beamline where the SC is located via a series of folding and focussing mirrors. The total path length of the VLE is $\approx$ 25 m, the reader should refer to [4] for further details.

In the diagnostics beamline the visible SR propagates through the input optics and is focussed onto the SC. Inside the SC, visible SR photons are converted to electrons by the photocathode. Electrons are deflected in two directions (horiz. (x) and vert. (y)) within the streak tube. At the end of the streak tube electrons are converted to photons via a phosphor screen. The photons undergo another conversion to electrons as they pass through the intensifier. At the end of the intensifier a second phosphor screen converts the electrons to photons. The readout unit consists of a series of lenses to image the phosphor screen onto the cooled CCD camera for readout. In Figure 1 a schematic overview of the system is illustrated.

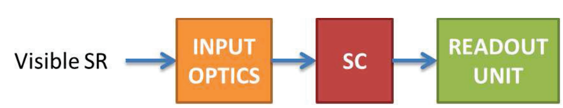

Figure 1: Schematic overview of the streak camera system.

A typical streak camera image with both deflections enabled is shown in Figure 2. The fast 250 MHz sweep and slow sweep run along the horizontal and vertical axes respectively as shown.

To obtain an accurate bunch length measurement the streak image is deconvolved with the PSF (see Figure 3) using the Richardson-Lucy algorithm [5]. The PSF is the measured spot size of the incident light on the SC with both deflections disabled. Next, each row of the deconvolved streak image is fitted with a Gaussian to obtain the r.m.s. bunch length in units of pixels. The bunch length is then converted from units of pixels to picoseconds using the calibration measurement in ps/pixel.

The reader should note that to a first approximation, and assuming the PSF width and bunch profile are Gaussian, the contribution of the PSF width to the bunch length measurement is added in quadrature. The contribution of the PSF to

ISBN 978-3-95450-176-2

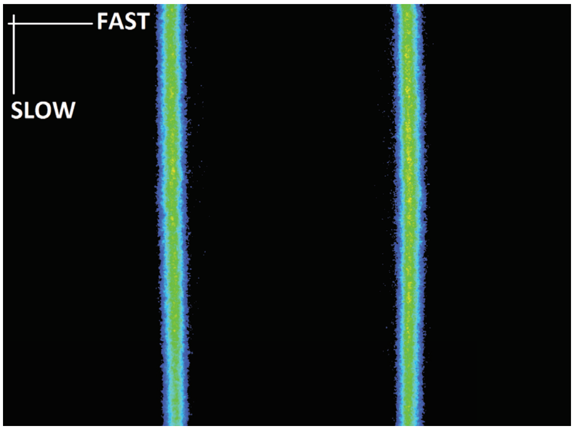

Figure 2: Typical streak camera image in low alpha.

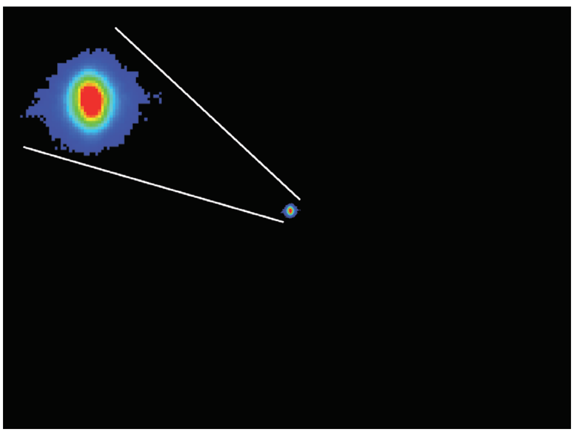

Figure 3: Typical PSF image with zoomed in ROI shown in top left.

the measured bunch length is shown in Eq. 2 where σ_{bunch} is the real r.m.s. bunch length, σ_{meas} is the measured bunch length and σ_{PSF} is the PSF width.

$$\sigma_{bunch} = \sqrt{\sigma_{meas}^2 - \sigma_{PSF}^2} \tag{2}$$

INPUT OPTICS UPGRADE

For SR studies using the single bunch low alpha beam mode, the input optics for the SC must be optimised to:

1. Propagate the maximum available light intensity to the SC.
2. Focus the incident SR beam to obtain a minimum PSF spot size at the SC.

In Figures 4 and 5 the layout of the previously implemented reflective input optics [6] and corresponding 2D-Gaussian fitted PSF image are shown respectively. The visible SR beam delivered from the VLE is somewhat astigmatic. It was also observed that after propagating through the previously implemented input optics more astigmatism was introduced. In Figure 5 the SC was longitudinally positioned in the horizontal focal plane to ensure the smallest PSF width along the fast sweep axis. With these input optics and astigmatism, the PSF could only be focussed in one

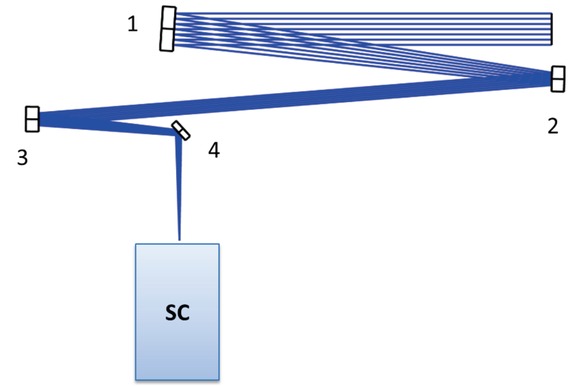

Figure 4: Original reflective input optics where (1) is concave parabolic mirror, (2) is a convex spherical mirror, (3) is a concave spherical mirror and (4) is a flat folding mirror.

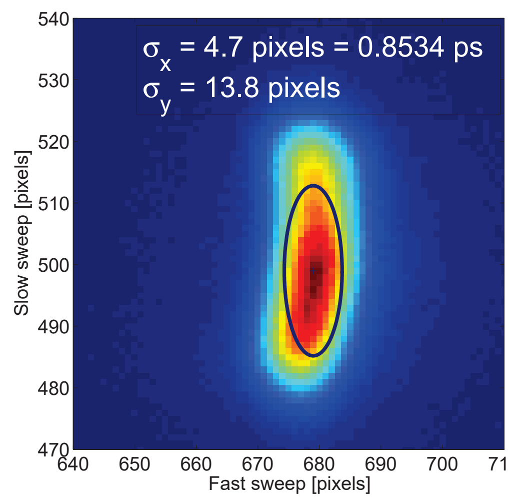

Figure 5: PSF acquired using the previously implemented reflective input optics.

direction. Therefore although the PSF contribution would be small for the bunch length measurements along the fast axis, blurring due to overlap along the slow axis reduced the ability to study dynamics along the slow (typically μs to ms scale) axis.

To obtain a small circular PSF a pinhole was inserted into the input optical system. The previously implemented reflective input optics shown in Figure 4 were relocated further upstream relative to the SC and were used to focus the almost-collimated SR beam onto the pinhole aperture for maximal light intensity.

The pinhole was imaged to the SC using two 90° off-axis parabolic (OAP) mirrors as shown in Figure 6. With a totally reflective optical system the maximum available light intensity could be propagated to the SC and the inclusion of a pinhole aperture provided the minimum ($\sigma_x \approx 0.7$ ps) circular PSF spot size as shown in Figure 7.

Due to the beam astigmatism, the PSF width along the fast axis could be favoured by adjusting the longitudinal position

ISBN 978-3-95450-176-2

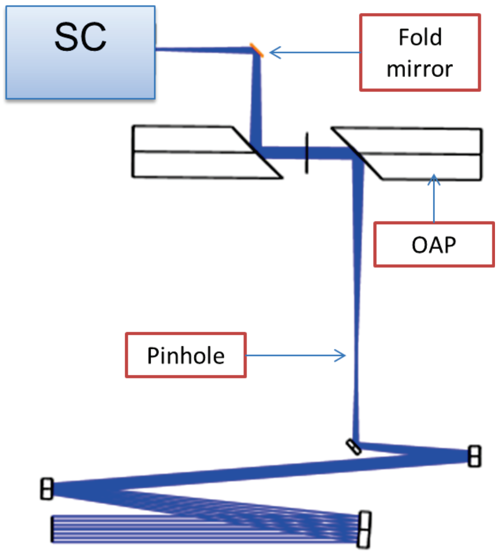

Figure 6: Layout of the upgraded reflective input optics.

of the streak camera. This explains the fit results shown in Figure 7 where the PSF width σ_x along the fast axis is slightly smaller than that along the slow axis σ_y.

The previously implemented reflective optics were left unchanged such that a roll-back could be done easily if required. However, due to the astigmatism introduced it may be preferable to replace this section of the input optics with a simpler single 90° OAP mirror.

The last element of the input optics is a folding mirror mounted on a gimbal holder to allow final alignment adjustments of the incident beam on the SC. The photocathode of the SC has a 2 mm × 2 mm central sweet spot within which the PSF should be located [3].

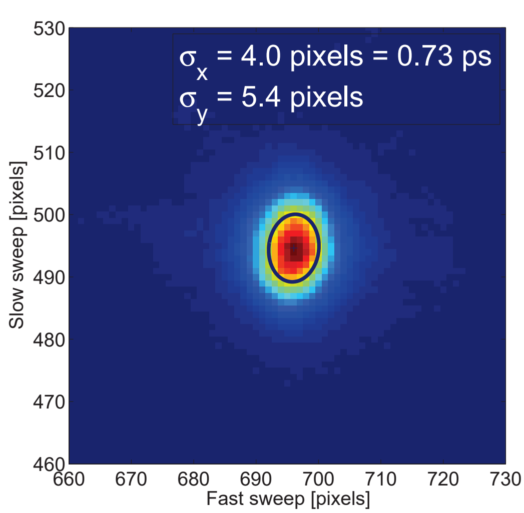

Figure 7: PSF acquired using the upgraded reflective input optics.

CALIBRATION

For bunch length measurements the dual sweep calibration of the SC must be known to a high degree of accuracy. Optical delay lines are most commonly used for SC timebase calibration. One such method is to split a single laser pulse into a train of identical pulses each taking a slightly longer path length and thus having different optical delays. The optical delays introduced are known and can therefore be compared to those measured within the streak image thus providing timebase calibration [7].

Including an optical delay line for the SR beam or for a separate laser source is often time-consuming due to the numerous degrees of freedom and accuracy required. Rather than delaying the arrival time of the incident pulse relative to the fast sweep deflection by a known amount, the same result can be achieved by delaying the fast sweep deflection relative to the arrival time of the incident pulse. For SR, the arrival time of the incident pulse is fixed by the parameters of the storage ring (i.e. the master oscillator frequency) and path length changes due to thermal drifts of the VLE and input optics happen on much longer timescales so can be considered negligible on the order of milliseconds.

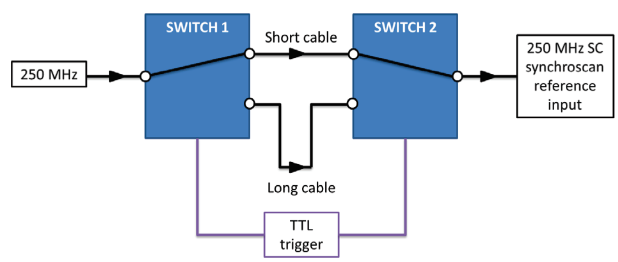

Figure 8: Illustration of the electrical delay introduced using PIN diode switches and cables of different lengths for the fast deflection signal.

In Figure 8 the principle of using the electrical delay difference between two cables of different lengths is illustrated. The 250 MHz signal is the input for the fast deflection unit of the SC. A waveform generator provides a square wave with a specified frequency which triggers the Mini-Circuits PIN diode switches such that the 250 MHz signal travels either via the short or the long cable. This is observed as a characteristic zigzag within the SC image as shown in Figure 9 where the electrical delay is $<$ 20 ps. It should be noted that the calibration can be disabled by simply disabling the output on the waveform generator.

The left and right streaks of the acquired images are analysed separately. Each row of the streak is Gaussian-fitted and the centroid positions are recorded in units of pixels. By taking the mean time shift between the two extreme centroid positions of the zigzag pattern, as denoted by the arrow between the red dashed lines in Figure 9, the electrical delay measured by the SC is obtained in units of pixels.

To obtain calibration values in units of ps/pixel for the left and right streaks the electrical delay must be quantified independently. The electrical delay due to the difference

ISBN 978-3-95450-176-2

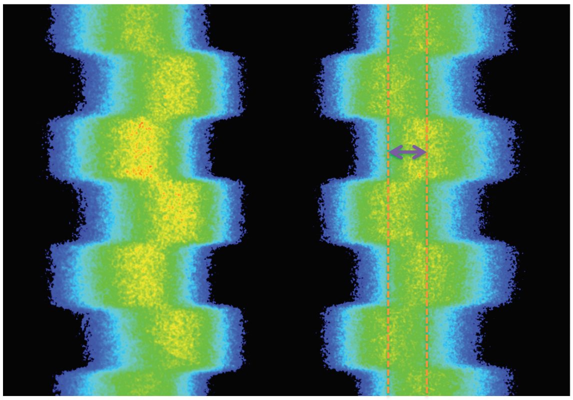

Figure 9: Streak camera calibration image taken in normal user beam where the separation between the dashed red lines is the measured delay used for calibration of the fast timebase. The slow timebase may be calibrated using the period of the square wave.

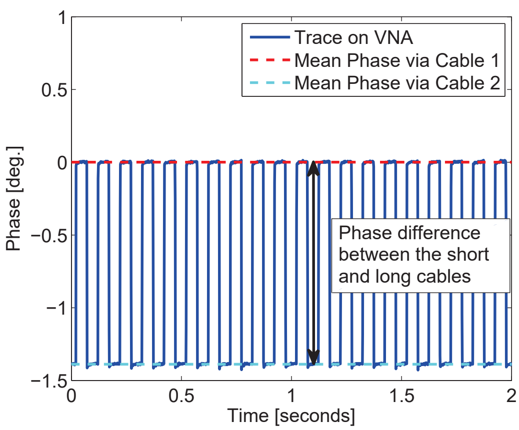

Figure 10: A plot of the 250 MHz VNA trace (blue line) with 10 Hz switching frequency between the short and long cables where the mean phase delays for each cable are shown by the dashed lines.

between the two cable lengths was measured using a Vector Network Analyser (VNA) as shown in Figure 10.

The electrical delay was obtained using the reported phase delay difference between the two cables. Given the phase delay θ in units of degrees, the electrical delay δ_{real} in picoseconds may be calculated using Eq. 3 where $T = 4000$ ps in our case for the 250 MHz deflection signal. Using this system the mean electrical delay was (15.4320 ± 0.0023) ps.

$$\delta_{real} = \frac{T}{360°} \cdot \theta \tag{3}$$

For maximum precision of the phase measurements the VNA was set up with a bandwidth (BW) of 1 kHz for the intermediate frequency (IF) while measuring at a fixed frequency of 250 MHz. Statistics are gathered from 1600 data points of a 2 seconds long trace. However, the narrow IF bandwidth required a low switching rate of 10 Hz.

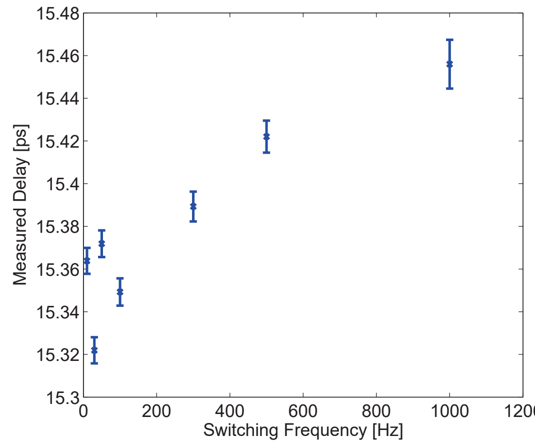

Figure 11: A plot of the measured electrical delay using the VNA for different trigger frequencies provided by the waveform generator. Data points with corresponding standard errors are denoted by crosses and errorbars.

It should be noted that in order to calibrate the timebases of the SC, a trigger frequency on the order of kHz is required. To this end, the VNA was set to a higher IF BW of 10 kHz. The electrical delay was measured for different frequencies as shown in Figure 11. The variation of the electrical delay with switching frequency over a range of 10 Hz - 1 kHz is $< 1\%$.

Given the known electrical delay and the measured time shift from the SC image δ_{SC} in pixels, the fast timebase calibration k_{fast} in units of ps/pixel may be calculated using Eq.4. For the SC at DLS, the fast deflection calibration is regularly measured to four decimal places and varies within the range of 0.17 - 0.20 ps/pixel.

The slow timebase calibration k_{slow} may be obtained by comparing the measured period of the square wave in the SC image (along the slow axis) with the expected period set by the waveform generator (see Figure 9).

$$k_{fast} = \frac{\delta_{real}}{\delta_{SC}} \tag{4}$$

CONCLUSION

For sub-ps bunch length measurements the optimisation of the input optics and calibration of the timebases of the streak camera must be performed.

At DLS, the input optics to the SC have been upgraded to work with white beam and to ensure a high resolution in both the fast and slow sweep directions through the reduction of the PSF spot size using a pinhole aperture. Operation in the low-alpha single-bunch beam mode for SR studies requires all elements in the input optical system to be reflective (vs refractive) to ensure maximum light intensity at the SC and to avoid pulse lengthening due to chromatic dispersion. With these upgraded input optics an r.m.s PSF spot size $\sigma_{PSF} \approx$ 0.7 ps could be achieved.

ISBN 978-3-95450-176-2

An example of the performance of the upgraded SC system is shown in Figure 12. Here the SC bunch length measurements (blue) are plotted against bunch current. The theoretical zero current bunch length is also shown (red). The SC data is in good agreement with the theory and bunch lengths < 2 ps have been measured.

In this report, a simpler method of timebase calibration of the SC using an electrical delay setup is presented. With this method calibration information is contained within the SC images. Calibration measurements can be performed simultaneously with data acquisition to ensure the calibration values are valid for the time at which the data was acquired.

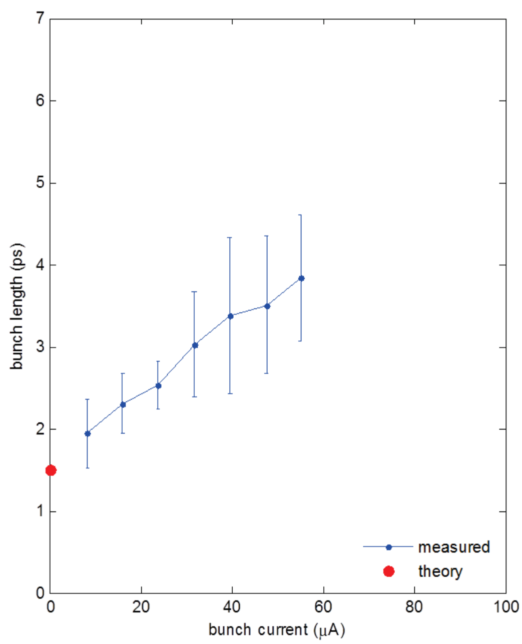

Figure 12: A plot of bunch length at various bunch currents in single bunch low alpha mode at 3.4 MV, $\alpha = -4.6 \times 10^{-6}$ and $f_s = 460$ Hz [8]. The error bars indicate the standard deviation over the ≈ 800 individual profiles analysed in each streak image.

REFERENCES

[1] C.A. Thomas et al., “Investigation of Extremely Short Beam Longitudinal Measurement with a Streak Camera”, TUPB41, *Proceedings of DIPAC09*, Basel, Switzerland (2009).

[2] I.P.S. Martin et al., Phys. Rev. ST Accel. Beams 14, 040705 (2011).

[3] Optronis GmbH website: `http://www.optronis.com/en/products/streak-cameras.html`

[4] C.A. Thomas et al., “Diagnostics Beamline Optimisation and Image Processing for Sub-ps Streak Camera Bunch Length Measurement”, TUPA42, *Proceedings of IBIC2012*, Tsukuba, Japan (2012).

[5] D.S.C. Biggs et al., Applied Optics 36, 8 (1997).

[6] C.A. Thomas et al., “Performance of a Streak Camera Using Reflective Input Optics”, MOPE081, *Proceedings of IBIC2010*, Kyoto, Japan (2012).

[7] S.L. Shapiro, *Ultrashort Light Pulses: Picosecond Techniques and Applications*, (Springer Science & Business Media, 2013), p29.

[8] I.P.S. Martin et al., “Reconstruction of Electron Bunch Motion During CSR Bursts using Synchronised Diagnostics”, MOPMA003, *Proceedings of IPAC2015*, Richmond, VA, USA (2015).

ISBN 978-3-95450-176-2